Journal of Fluorescence, Vol. 9, No. 4, 1999

Preparation and Entrapment of Fluorescently Labeled Proteins for the Development of Reagentless Optical Biosensors

John D. Brennan[1]

Received March 31, 1999; accepted April 28, 1999

A new class of reagentless optical biosensors are emerging based on the use of engineered proteins that are site-selectively labelled with a fluorescent reporter group. Such sensors can operate either by direct interaction of the analyte with the bound probe, or by generating a fluorescence response to an analyte induced conformational change in the protein. In this review, the preparation, characterization and use of fluorescently labelled proteins for the development of reagentless optical biosensors is described. Recent work involving the rational design of fluorescent protein biosensors, and efforts at characterizing the origins of responses from these systems is highlighted. An overview of the recent and potential future trends in this area is also given. Finally, methods of immobilizing such biomolecules for the development of reuseable sensors are described.

KEY WORDS: Reagentless optical biosensors; fluorescently labeled proteins; entrapment.

INTRODUCTION

Overview

The development of chemical sensors and biosensors is one of the most active areas of research within the field of analytical chemistry, as demonstrated by the number of reviews and monographs that are devoted to this subject [1–3]. The design of a biosensor, as illustrated in Fig. 1, is centered around a selective chemical or biochemical sensing region that is interfaced to, or incorporated within, a physical transducer. Analyte recognition in biosensors is most often achieved through the use of biological compounds that can react selectively with an analyte. The species which have been most widely used for this purpose are antibodies [4] and enzymes [5], owing mainly to their wide commercial availability and their ease of use. However, a number of other biological species have been used to impart selectivity to sensors, including peptides [6], molecular receptors [7], and regulatory proteins [8].

One of the major challenges in sensor development is the need to convert the interaction between the analyte and the protein, which itself is often not directly measurable [9], into a measurable signal. Several strategies have been employed to achieve this goal, including electrochemical detection strategies [10], semiconductor-based strategies [11], piezoelectric transduction methods [12], thermal methods [13], and optical methods based on absorbance [14], Raman [15], surface plasmon resonance [16], and fluorescence [17] techniques. The sensor is designed such that the binding of analyte to the protein mediates an analytical signal (i.e., electrical potential, current, oscillation frequency, scattering or luminescence intensity) in a manner that is proportional analyte concentration.

Reagentless Sensors

The vast majority of sensors that have been reported to date rely on antibodies and enzymes for selectivity.

[1] Department of Chemistry, McMaster University, Hamilton, Ontario, Canada L8S 4M1. e-mail: brennanj@mcmail.cis.mcmaster.ca

1053-0509/99/1200-0295$16.00/0

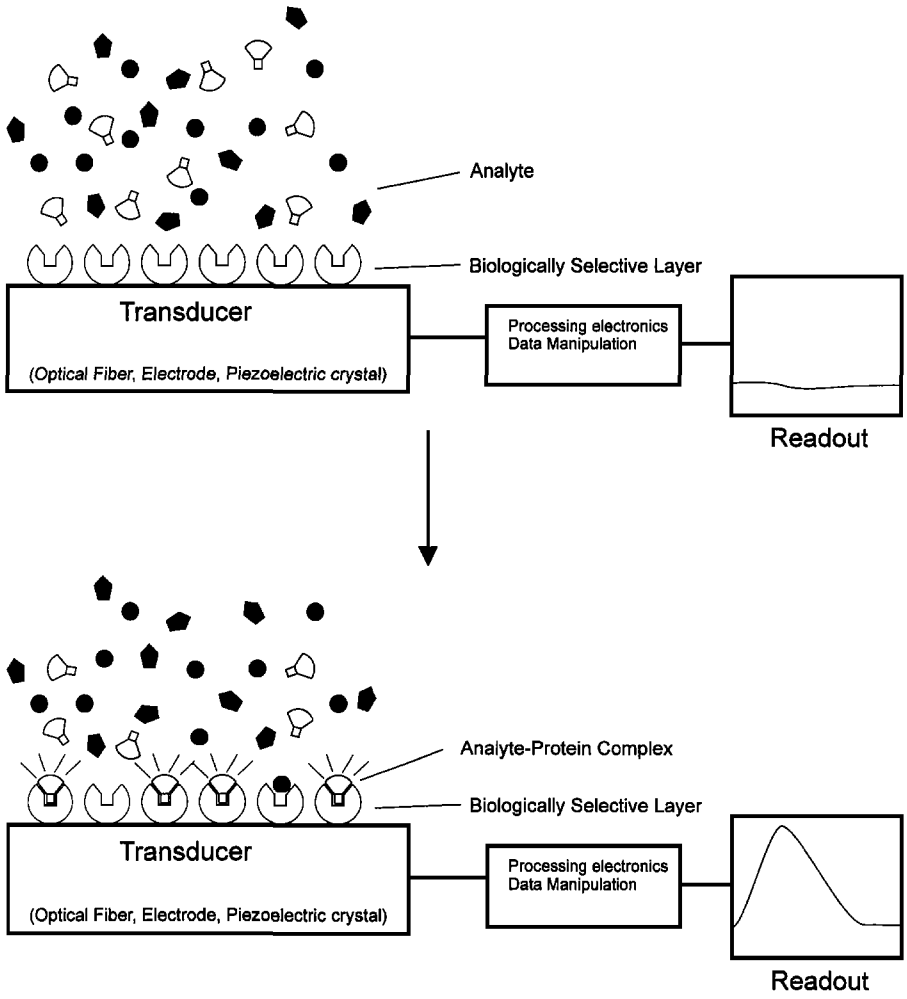

Fig. 1. Schematic design of a generic biosensor. The selective binding of the analyte to form an analyte–protein complex leads to the generation of an analytical signal which is converted to a readout.

Sensors based on such species monitor the formation of an antibody–analyte complex (usually by an optical or piezoelectric method) or measure the decline in analyte concentration or evolution of secondary products arising from an enzyme–analyte interaction (generally by electrochemical or optical methods). However, sensors that utilize these biorecognition elements often suffer from serious limitations. In the case of antibody-based sensors, the complexes formed with antigens are usually irreversible, relegating immunosensors to being single-use devices. Furthermore, it is often necessary to add various reagents, such as a fluorescently labeled analyte or a second antibody labeled with an enzyme or fluorophore, in order to obtain an analyte-dependent signal from an immunosensor. In the case of enzyme-based sensors, there is often a need to add multiple reagents (in addition to the analyte) in order to generate a signal from an enzyme–substrate reaction. Such species may include redox mediators, pH sensitive dyes, or reagents that form fluorescent complexes with evolved products. The need to add extra reagents in order to quantitate analyte concentration is a serious problem for sensor development, since these steps are both costly and time-consuming. Ideally, one should have a sensor where the analytical reporter group (i.e., redox site, fluorescent probe) is directly coupled to the biorecognition element. In such a case, the selective binding of an analyte to the sensor surface results in a direct or indirect change in the properties of the reporter group, without the need for the addition of any extra compounds. Such a design is termed "reagentless," since only the analyte needs to be present to produce a signal change.

One of the recent advances in the field of biosensor design, which directly addresses the issue of reagentless

sensing, has been the use of fluorescently labeled enzymes [18], antibodies [19], peptides [20], and regulatory proteins [8] as selective recognition elements. In many cases, these proteins are engineered to allow site-selective labeling with an environmentally sensitive fluorescent probe or are linked to a green fluorescent protein (GFP) to form a chimera. Binding of the analyte results in either a direct signal owing to specific interactions with the probe or an indirect signal wherein a conformational change in the protein alters the environment of the probe or GFP, producing a measurable change in the fluorescence properties of the protein (intensity, emission wavelength, anisotropy, or efficiency of fluorescence resonance energy transfer; FRET). Using this strategy, it is possible to measure the concentration of nonfluorescent analytes, and there is no need to add any extra reagents in order to generate a signal. In addition, biorecognition elements such as regulatory proteins are attractive for sensor development since they usually bind analytes reversibly and have binding constants that permit detection of analytes over a concentration range spanning picomolar up to millimolar levels.

In this article, the various strategies for developing reagentless fluorescence sensing schemes are outlined. In many cases, such schemes make use of site-directed mutagenesis techniques to improve reagentless sensor performance. Some of the most recent developments in this field are highlighted, and the advantages and limitations of such sensors are outlined. Finally, methods for the immobilization of such proteins to sensor surfaces are described, with particular emphasis on emerging techniques involving the entrapment of proteins into sol-gel-processed glass matrixes.

REAGENTLESS FLUORESCENCE SENSING STRATEGIES

Enzyme-Based Systems

An immense amount of research has been done in the area of enzyme-based fluorescent biosensors; however, this review outlines only those systems that meet the criteria for reagentless sensing. The systems fall into those which utilize the fluorescence of a bound cofactor, such as the flavin adenine dinucleotide (FAD) or flavin mononucleotide (FMN), and hence do not require protein engineering steps, and those that use protein engineering to insert a reactive amino acid residue in order to allow a fluorescent probe to be site-selectively attached to the enzyme, thereby allowing reagentless detection of substrate or cofactor binding.

The changes in FAD fluorescence upon interaction of a substrate with a redox enzyme, such as glucose oxidase (GOx) or cholesterol oxidase (ChOx), was initially investigated by Weber [21], and Visser later proposed and demonstrated a model for such changes [22]. When FAD is present in a protein such as GOx, it can undergo a redox reaction wherein it interconverts between FAD and $FADH_2$. The reduction of FAD results in a reversible increase in the intensity of emission that is proportional to analyte concentration.

The first use of FAD-containing proteins for sensor development was described by Wolfbeis and Trettnak [23]. GOx [23,24] and ChOx [23], which both have a bound FAD cofactor, and lactate monooxygenase (LMO) [23,25], which has a FMN cofactor, were examined. Changes in the fluorescence of the flavin moiety were capable of detecting substrate (glucose, cholesterol, or lactate, respectively) over the range of 0.5 to 3.0 m*M*. An advantage of this approach was that the signal generated was reversible. Another advantage is that the FAD moiety has an excitation maximum at 460 nm, which coincides almost exactly with the maximum output wavelength of a blue LED (460 nm) [26], and also allows excitation with a He–Cd laser source at 441.6 nm. Disadvantages involved mainly the low quantum yield of FAD, the small change in intensity of FMN and FAD upon undergoing redox reactions, the relatively slow response time (up to 30 min at low concentrations of substrate), and the very small dynamic range over which these cofactors were sensitive. It remains to be seen whether such proteins become viable platforms for reagentless sensing.

A promising alternative route to obtain a reagentless enzyme-based sensor is to use a fluorescent inhibitor that binds to the protein only in the presence of a specific cofactor. Thompson and Jones initially demonstrated this approach for sensing Zn(II), based on the binding of a dansylamide inhibitor to the Zn(II) cofactor after the cofactor had bound to the active site of carbonic anhydrase [27]. Initial studies used the inhibitor in solution and utilized fiber-optic detection. In this case, the concentration of metal ion over the range of 50 to 1000 n*M* was found to be proportional to the ratio of fluorescence intensities at two emission wavelengths, corresponding to emission from the bound and free inhibitor.

More recent work by Thompson and co-workers [28,29] has focused on the use of fluorescence anisotropy as an analytical signal. The anisotropy of a label (r) is determined both by the rotational correlation time of the probe (ϕ) and the fluorescence lifetime of the probe (τ), according to the following equation:

$$r = \frac{r_0}{1 + \tau/\phi} \quad (1)$$

where r_0 is the limiting anisotropy of the probe obtained in the absence of rotational motion. The anisotropy is determined by exciting the sample with plane polarized light and measuring the emission intensity of light polarized along axes, which are parallel ($I_{\|}$) or perpendicular ($I_{\perp}$) to the incident beam, and is given by the following ratio:

$$r = \frac{I_{\|} - I_{\perp}}{I_{\|} + 2I_{\perp}} \quad (2)$$

The advantage of this technique is that anisotropy is inherently ratiometric and, thus, is insensitive to problems associated with photobleaching, leaching of dye, changes in excitation intensity, or other optical effects.

Anisotropy-based sensing used the aminobenzoxadiazole mercaptoethanol (ABD-M) probe [28], which was synthesized and used to determine the amount of free Zn (II) in solution. As in the earlier work, the sensor worked by using carbonic anhydrase to bind to Zn(II) in solution. Zn(II) binding was followed by binding of the sulfonamide of free ABD-M, present in solution, to the bound Zn(II), resulting in a large decrease in the rotational correlation time for the probe and an increase in steady-state anisotropy. Using this approach, Zn(II) could be detected at picomolar levels, with a dynamic range of 2 orders of magnitude. The key problems with this strategy were the need to add the ABD-M as an extra reagent, and the slow response times, which in some cases were on the order of hours.

The most recent work from the Thompson laboratory has extended the technique to a reagentless format that is suitable for the detection of several metal ions, including Zn(II), Cu(II), and Co(II) [30]. This was accomplished by covalently binding the sulfonamide probe to a cysteine residue, which was placed near the active site via site-directed mutagenesis. The detection of Cu(II) and Co(II) relied on quenching of the fluorescence of the ABD probe, bound to a F131C mutant. The quenching produced a substantial reduction in the fluorescence lifetime, and hence an increase in the observed anisotropy, even though the rotational correlation time did not change significantly. Using this approach, Co(II) could be detected between 10 and 1000 n*M*, while Cu(II) could be detected from 0.01 to 50 p*M*. For detection of Zn(II), a H64C mutant was used. In this case, binding of Zn(II) did not change the fluorescence lifetime; however, the complexation of the probe to the bound Zn(II) resulted in a substantial increase in the rotational correlation time of ABD, producing an increase in steady-state anisotropy. Zn(II) could be detected over the range spanning 1 p*M* to 10 n*M*. This work demonstrated the utility of reagentless sensing of cofactors, since the probe did not have to be added to the protein, as was the case in the earlier examples. In addition, the use of protein engineering methods allowed for optimization of the probe location, maximizing the performance of the sensor.

Reagentless Immunosensors

In addition to reagentless enzyme-based systems, there has been some work done on the development of reagentless sensors that utilize antibodies. As indicated earlier, these biomolecules have the advantage of good specificity, availability for a wide range of analytes, and ease of use. The primary difficulty lies in the irreversible nature of antibody–antigen complexes, and this limits their utility for continuous sensing applications. However, some work has been done to make these devices more amenable to reagentless sensing, and these advances are outlined here.

One of the first developments for reagentless immunosensor design was described by Bright and co-workers in 1990 [19]. In this work, anti-HSA was incubated with HSA to block the active site of the antibody. The complex was then nonselectively reacted with dansylamine to place a solvent-sensitive fluorophore near the active site of the antibody. Removal of HSA was then done and the labeled antibody was immobilized near the distal tip of an optical fiber. The binding of HSA resulted in a large blue shift in the dansyl emission wavelength and an increase in emission intensity that was directly related to HSA concentration. The sensor could be regenerated using a cheotropic solution and reused up to six times before significant changes in the fluorescence response were observed.

The use of labeled antibodies has continued to evolve in recent years. For example, myoglobin has been detected in a reagentless format using the antimyoglobin antibody, which was labeled with the fluorescent dye cascade blue [31]. The labeled antibody was placed into a polyacrylamide gel layer at the distal tip of an optical fiber. Binding of myoglobin resulted in fluorescence resonance energy transfer from the cascade blue label to the heme group of the myoglobin. Using this approach, myoglobin could be measured in a reagentless fashion with a LOD of 83 μg·L, and with a response time between 15 and 130 min.

Other examples of potential formats for both heterogeneous, homogeneous, and reagentless immunosensors have been reviewed by Price and co-workers [32] and by Hock [33]. Of the emerging strategies for immunosensor

development, one of the most exciting developments is the use of protein engineering methods to prepare single-chain antibodies suitable for biosensor purposes. Hellinga has demonstrated that single chains comprising the variable region of the antigen binding fragment (scFv) can be site-selectively modified with a peptide which has a high affinity for streptavidin [34]. This allowed immobilization of the scFv onto a streptavidin-coated surface with a high degree of orientational control. The immobilized antibody was able to bind a fluorescently labeled phosphorylcholine analogue, as detected by total internal reflection fluorescence measurements. In the future, it should be possible to engineer the scFv with a fluorescent probe placed in a well-defined position near the binding site, such that the binding of an antigen will cause a measurable change in the emission properties of the label. Benkovic and co-workers have demonstrated a preliminary version of this strategy, wherein an intrinsically fluorescent scFv was used to generate a reagentless fluorescence response that was related to the binding of micromolar concentrations of Zn(II) [35].

Regulatory Peptides and Proteins

One of the most exciting and active areas of research within the biosensors field is the use of fluorescently labeled regulatory peptides and proteins for the development of reagentless sensing schemes. In such systems, the binding of an analyte either causes a direct change in the emission properties of a covalently attached fluorescent moiety, or results in an indirect change in fluorescence, which is mediated by a conformational change within the biomolecule. Examples of the various strategies are summarized in Table 1 and are outlined in more detail below.

Direct Sensing

Numerous fluorescence-based sensors have been developed which rely on a direct alteration in the environment surrounding the probe upon binding of analyte. Many of these systems are designed such that the analyte is simply a known fluorescence quencher, such as O_2, Co^{2+}, or I^-, which does not need to bind to the protein in order to produce a signal. However, there are some recent examples of direct, reagentless monitoring of analytes where the analyte binds selectively to the protein, causing a direct change in the emission of an attached probe. Examples include the use of a fluorescently labeled fatty acid binding protein for detection of fatty acids [36], the use of a labeled myosin light chain to examine myosin phosphorylation events [37], and the use of cytochrome *c'* for fluorimetric detection of nitric oxide [38].

The detection of free fatty acids (FFA) used a fatty acid binding protein (FABP), which was site-selectively labeled with the solvent sensitive probe acrylodan (Ac) at Lys 27 [36]. Binding of fatty acids to the Ac-labeled protein resulted in a displacement of the Ac probe from the hydrophobic fatty acid binding pocket, producing a 55% decrease in emission intensity that was accompanied

Table I. Examples of Regulatory Protein Systems and Probes Used for Reagentless Sensing

Protein system	Label(s) used	Method of signal generation	Analyte measured	Ref. No.(s.)
Fatty acid binding protein	Acrylodan	Emission intensity ratio	Free fatty acids	36
Cytochrome *c'*	Fluorescein	Quenching by nitric oxide	Nitric oxide	38
Zinc-finger domains	Dansyl	Emission ratio	Zn(II)	20
	Lissamine/fluorescein	FRET		44
Parvalbumin	Acrylodan	Emission intensity	Ca(II)	45
Calmodulin	Fluorescein	Emission intensity	Ca(II)	47
Troponin C	IAANS	Emission intensity	Ca(II)	48
MLCK	GFP	FRET	Ca^{2+}-loaded CaM	50
CaM-M13 chimera	BGFP/RGFP	FRET from BGFP–CaM to RGFP–M13	Ca(II)	52
cAMP-dependent kinase + regulatory subunit	Fluorescein + rhodamine	FRET from fluorescein to rhodamine	cAMP	53
Maltose binding protein	NBD, acrylodan	Emission intensity	Maltose	56,64
Glucose binding protein	NBD, acrylodan	Emission intensity	Glucose	65
Phosphate binding protein	MDCC, acrylodan	Emission intensity	Inorganic phosphate	57–61
P-glycoprotein	MIANS	Quenching of intensity	Drug compounds or ATP	54
Insulin receptor	Tryptophan	Emission intensity Rotational anisotropy	Insulin	55
SH2-SH3 chimera	Dansyl	Emission intensity	Bridged SH2–SH3 binding peptide	69

by a 35-nm red shift in the emission maximum, as well as a substantial decrease in the rotational anisotropy of the probe. Using the Ac-labeled FABP (denoted ADIFAB), it was possible to monitor the release of fatty acids from rat basophilic leukemia cells upon the addition of ionomycin. By measuring the ratio of emission intensities from free and bound Ac, artifacts arising from light scattering by the cells were effectively eliminated. In addition, it was possible to measure the free fatty acid content rather than the total fatty acid content, as measured using other techniques which rely on radiolabeled fatty acids.

Detection of myosin II light-chain phosphorylation by myosin light-chain kinase (MLCK) utilized an engineered myosin light chain containing a single cysteine at position 18 [37]. This site was selectively labeled with acrylodan to place a reporter group next to the site of phosphorylation. Phosphorylation of serine 19 resulted in a 28-nm red shift in the emission maximum and a 60% decrease in intensity, and it was suggested that an increase in the local charge in the vicinity of the Ac label produced the observed changes in fluorescence. Injection of the labeled protein into living fibroblasts and smooth muscle cells was also done, and the labeled protein demonstrated a phosphorylation-dependent fluorescence response. The major drawback of the new sensor was the requirement for excitation in the UV region of the spectrum. This requirement resulted in difficulties with cell autofluorescence and led to a higher propensity for photobleaching.

The final example of the direct sensing strategy was the use of cytochrome c' (Cyt c') for the detection of nitric oxide [38]. The binding of NO to the pentacoordinate Fe site in Cyt c' resulted in a change in the emission characteristics of the porphyrin group. In cases where the porphyrin ring was directly excited at 530 nm, the addition of NO at levels up to 1 mM resulted in substantial quenching of the intensity at 640 nm and produced a blue shift in the emission wavelength maximum. While this approach worked, it suffered from poor signal-to-noise characteristics, providing poor detection limits. To overcome this problem, the Cyt c' was nonselectively labeled with the succinimidyl ester of 4-carboxy-3,4,6 trifluoro-2′,7′-difluorofluorescein, whose emission overlaps the absorbance band of the protein so that the label acts as a donor while the heme group acts as an acceptor for FRET. The labeled protein showed a similar sensitivity for detection of NO but had a substantially improved LOD, which was determined to be 20 μM. An interesting aspect of this work was that the detection of NO was done with protein that was trapped in a polyacrylamide gel at the end of a nonooptrode, measuring only 200 nm in diameter at the tip. Based on the small volumes that can be monitored with such a device (stated to be as little as 10 pL), it should be possible for the device to measure as little as 200 amol of NO under optimal conditions, although this remains to be demonstrated.

Indirect Sensing

A much more common route for preparing reagentless sensors involves indirect alterations in fluorescence upon analyte binding. This goal is achieved by placing a fluorescent probe into a region of the biomolecule that undergoes a change in local environment as a result of an analyte-induced conformational change. In such as case, an analyte-dependent fluorescent signal is generated that is determined by changes in protein conformation and is fully reversible. Furthermore, since the location of the probe is physically removed from the binding site, it is possible to modify each part of the protein independently, producing a wider range of opportunities for sensor optimization.

There are many proteins that undergo conformational changes on binding with analyte, and these display selectivity for a wide array of analytically interesting compounds. The mechanisms of protein motions have been reviewed by Gerstein *et al.* [39], while the use of such proteins for developing fluorescence-based biosensors has been reviewed by Giuliano *et al.* [8,40] and Hellinga and Martin [41]. In general, proteins can undergo either a shear motion, wherein one domain slides over another on analyte binding, or a hinge motion, wherein two domains come together on ligand binding, as shown in Fig. 2. Examples of shear motion proteins (with ligands in parentheses) include [39] citrate synthase (oxaloacetate), hexokinase (glucose), alcohol dehydrogenase (ethanol), and trp repressor (tryptophan). Examples of hinge motion proteins include the periplasmic binding proteins (PBPs), of which about 20 are known [39]. Examples include the maltodextrin binding protein (maltose), the glucose/galactose binding protein (glucose), and proteins which bind ligands such as cysteine, glutamine, inorganic phosphate, and vitamin B_{12}. Other hinge proteins include calmodulin (Ca^{2+}), lactoferrin (Fe), cAMP-dependent protein kinase (cAMP), and others. Finally, immunoglobulins are an important class of proteins which can show extensive domain movement on binding of antigens (up to 50° based on a ball & socket joint which forms an interface between the domains [42]), although to date no reports have emerged which make use of this property for signal development.

Peptide-Based Systems. One of the systems in which analyte binding induces a major conformational change is for Zn(II)-binding polypeptides (referred to as zinc finger domains). In the absence of Zn(II), the zinc

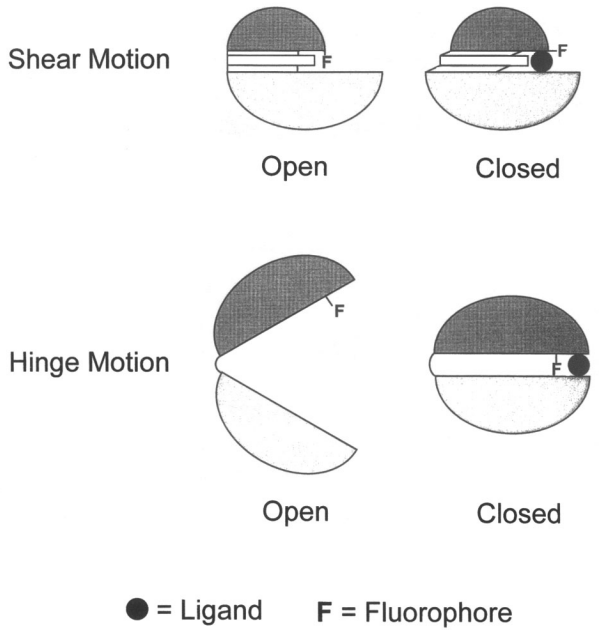

Fig. 2. Examples of protein conformational motions involving (a) shear and (b) hinge movements. The binding of the ligand results in a change in the location and hence environment of the attached fluorescent probe.

fingers are disordered. However, upon binding of Zn(II), coordination to His and Cys residues promotes the formation of a defined tertiary structure, including a hydrophobic cluster. Walkup and Imperiali synthesized a Zn(II) binding polypeptide with a dansyl group placed within the cluster of residues forming the hydrophobic pocket, and the resulting peptide showed a significant fluorimetric response to Zn(II)-induced structural changes [20]. Ratiometric analysis, using emission wavelengths at 650 nm (Zn^{2+}-free) and 525 nm (Zn^{2+}-loaded) showed that the response was linear over the range from 0.1 to 1 m*M* Zn(II) and that the response was fully reversible. In later work, Imperiali and co-workers showed that the separation of the fluorescent reporter group from the Zn(II) binding domain provided the advantage of being able to manipulate each part independent of the other [43]. In this work, it was demonstrated that the affinity of the metallopeptide for binding of Zn(II) could be manipulated by altering the Zn(II) binding domain, without affecting the performance of the attached fluorophore. Using this approach, dissociation constants for binding of Zn(II) ranging from 7 p*M* to 65 n*M* were achieved.

Godwin and Berg reported a Zn(II) sensing strategy based on a principle similar to that described above [44]. In this case, the peptide was selectively labeled at one site with lissamine, and at another with fluorescein. Binding of Zn(II) resulted in a conformational change that brought the two probes into closer proximity, increasing the energy transfer efficiency from fluorescein to lissamine. The ratio of emission intensities at 521 and 596 nm was sensitive to Zn(II) binding in the concentration range from 0.1 to 1.0 m*M*. The main advantage of this particular sensing strategy was the ability to excite between 430 and 480 nm, which eliminated biological autofluorescence and which was compatible with the output of both a He–Cd laser and a blue LED.

Ca^{2+} Binding Proteins. While peptide-based reagentless sensors have been reported, the development of fluorescent protein biosensors is far more common. One of the earliest uses of a fluorescently labeled protein for monitoring analyte-induced conformational changes was based on the labeling of Ca^{2+} binding proteins with acrylodan, as reported in 1983 by Prendergast and co-workers [45]. This work demonstrated that the newly synthesized probe 6-acryloyl-2-(dimethylamino)naphthalene (acrylodan, Ac) could be selectively bound to the free cysteine of parvalbumin or troponin C at a 1:1 ratio of probe to protein and that binding of Ca^{2+} to the apoprotein resulted in a red shift in the emission maximum and a decrease in quantum yield for both proteins. The response was consistent with the relatively hydrophobic probe being sequestered within a hydrophobic pocket or domain in the apoprotein but being partially extruded into the solvent as a result of the Ca^{2+}-induced conformational change. Hence, the signal change required to develop a reagentless protein-based optical sensor for Ca^{2+} was realized.

Since this pioneering work, the idea of utilizing analyte-induced conformational changes of fluorescently labeled proteins to generate analytical signals has been further investigated by a number of groups. Initial studies used nonselective labeling methodologies and did not require protein-engineering steps. For example, in 1990 Taylor and co-workers used a merocyanine-labeled calmodulin (meroCaM), to detect CaM activation in cells [46]. The lysine residues of the protein were randomly labeled (CaM has a total of eight Lys residues), but the labeling conditions were such that a probe:protein ratio of 1:1 was obtained. The labeled protein showed Ca^{2+}-binding characteristics that were similar to that of the unlabeled protein and provided a reversible fluorescence change upon binding of nanomolar levels of Ca^{2+} while being insensitive to millimolar levels of Mg^{2+}. However, the use of the merocyanine dye resulted in the need to measure a ratio of emission intensities at two excitation wavelengths in order to produce a signal, making it unsuitable for sensors that utilize excitation sources that operate at a single, fixed wavelength.

In later work, Bachas and co-workers reported a Ca^{2+} sensor that was based on fluorescently labeled cal-

modulin, which was trapped at the end of an optical fiber using a simple dialysis membrane [47]. Commercially available FITC-labeled calmodulin (F-CaM) was used, with the fluorescein conjugated to the protein though any one (or more) of the eight lysine groups present, resulting in a final probe:protein ratio of 0.8. The addition of Ca^{2+} resulted in a decrease in emission intensity from the labeled protein, although the exact basis of this change was not investigated. Using this strategy, Ca^{2+} could be detected over the range of 50 to 1000 n*M*, with no interference from Mg^{2+} at levels up to 10 m*M*. Ions which had similar ionic radii to Ca^{2+}, particularly Cd^{2+} and Eu^{3+}, did result in substantial interferences when present at levels of 500 μ*M*. The sensor response time was ~15 min, which is longer than is desirable for a working sensor. Another major problem was that the F-CaM leached through the dialysis membrane, limiting the working lifetime of the sensor to only one day.

More recent work with Ca^{2+}-binding proteins has involved the used of single Cys mutants of Ca^{2+} binding proteins such as troponin C or CaM, which actually goes back to the initial work of Prendergast [45]. The Cys can be site-selectively labeled with a variety of probes that are sensitive to Ca^{2+}-induced conformational changes. An example of this methodology is the labeling of single Cys mutants of cardiac troponin C to produce a Ca^{2+} sensor [48]. The protein has two naturally occurring Cys residues, at positions 35 and 84. Single Cys mutants were prepared and were labeled with (2-4′-(iodoacetamido)-anilino)naphthalene-6-sulfonic acid (IAANS), which absorbs at 320 nm. While both the Cys-35 and the Cys-84 forms were able to detect Ca^{2+}, the Cys-35 mutant showed a decreased Ca^{2+} binding affinity in site II, and the response to Ca^{2+} did not coincide with force generation in skinned muscle fibers. The Cys-85 mutant, on the other hand, was able to sense Ca^{2+} with an affinity similar to that of the native protein and showed excellent coincidence of Ca^{2+} levels and force generation. Hence, this study clearly showed that location of single Cys mutants has to be carefully chosen to minimize perturbations of protein structure or function which can alter it's response.

GFP-Labeled Ca^{2+} Binding Proteins. An interesting variant of the above studies involves the use of GFP-labeled proteins for detection of analytes. Numerous examples of this strategy have appeared and have recently been briefly reviewed by Tsien and Miyawaki [49]. A few key examples are presented here. Most strategies employing GFP-labeled proteins have utilized FRET as a means of generating a signal. An example of this is the use of a GFP-labeled CaM binding domain from MLCK to detect Ca^{2+}-loaded CaM in cells via an energy-transfer method [50]. Protein engineering was used to construct a chimeric CaM binding domain *in situ*, which was labeled on one end with the "blue" form of the green fluorescent protein (BGFP, $\lambda_{max,ex}$ = 382 nm, $\lambda_{max,em}$ = 448 nm) and at the other end with the "red" form of GFP (RGFP, $\lambda_{max,ex}$ = 495 nm, $\lambda_{max,\ em}$ = 509 nm). In the absence of CaM, or in the presence of apo-CaM, the GFP labels were in close proximity, resulting in substantial energy transfer. On binding of holo-CaM, the GFP-labeled CaM-binding domain adopted an extended conformation, spatially separating the BGFP and RGFP labels and decreasing the energy transfer efficiency. Using this method, it was possible either to detect Ca^{2+} by having an excess of apo-CaM available in the solution containing the fluorescent indicator protein (denoted FIP-CM_{SM}) or to detect holo-CaM directly.

A key disadvantage of the approach outlined above was that the two species had to be added to the solution (CaM and FIP-CM_{SM}), meaning that reagentless sensing of Ca^{2+} was not possible. In addition, it was possible that the labeled CaM binding domain could nonselectively associate with other hydrophobic proteins present in the cellular milieu. This problem was overcome by linking the C terminus of the FIP-CM_{SM} mutant (RGFP-MLCK-BGFP, where $MLCK_f$ is the CaM-binding fragment of MLCK) to the N terminus of CaMCN (C- and N-terminal regions exchanged) [51]. These chimeric proteins responded directly to changes in free Ca^{2+} through a change in the energy transfer efficiency between the two forms of GFP. The ratio of emission intensities at 440 and 505 nm allowed detection of Ca^{2+} over the range from 50 n*M* to 1 μ*M* with response times of under 1 s. The only major disadvantage was a pH dependence of the signal, which was due to the quenching of GFP fluorescence at pH values below about 6, and problems with autofluorescence when these species were used *in vivo*.

Miyawaki *et al.*[52] used a similar approach wherein the C terminus of CaM was linked to the M13 peptide (the 26-amino acid fragment of MLCK, which is responsible for binding to CaM) via a Gly–Gly spacer to form a chimeric protein. In this case, the BGFP was bound to the N terminus of CaM, while RGFP was bound to the C-terminal end of the M-13 peptide. Binding of Ca^{2+} by CaM resulted in a conformational change which caused an increased efficiency for FRET from the BGFP to the RGFP and, hence, an increase in the ratio of intensities at 510 vs 445 nm when excited at 380 nm. An advantage of the new protein, termed "cameleon-1," was that it was not able to bind to other hydrophobic proteins or endogenous calmodulin-binding sequences often found in eukaryotic cells. The chimeric protein showed a biphasic response to Ca^{2+}, which resulted in an extended range over which Ca^{2+} could be detected, spanning 100 n*M* up

to 100 μM. Several other mutants were prepared, one of which used a cyan GFP (CGFP $\lambda_{max,ex}$ = 433 nm, $\lambda_{max,em}$ = 470 nm) and a yellow GFP (YGFP $\lambda_{max,ex}$ = 495 nm, $\lambda_{max,em}$ = 525 nm), replacing the BGFP and RGFP, respectively. This shift of the excitation maximum from 381 to 433 nm substantially reduced the cellular autofluorescence and allowed the chimeric protein to follow antagonist- and agonist-induced changes in free Ca^{2+} concentrations when it was microinjected into mammalian cells or endoplasmic reticulum.

FRET-Based cAMP Sensor. An example of the use of FRET which did not involve GFP-labeled proteins was a fluorescence sensing strategy for detecting cAMP in single smooth muscle cells [53]. In this work, the catalytic subunit of cAMP-dependent protein kinase was nonselectively labeled with fluorescein, while the regulatory subunit was nonselectively labeled with rhodamine. In the absence of cAMP, the average distance between the fluorescein and the rhodamine probes was short, and hence the fluorescein was somewhat quenched due to energy transfer to rhodamine. Upon binding cAMP, the catalytic and regulatory subunits dissociated, resulting in the distance effectively increasing to infinity. This dissociation caused a decrease in rhodamine emission and an increase in fluorescein emission. This approach was able to detect free cAMP at concentrations ranging from 0.01 to 1.0 mM, with response times of the order of a few minutes. Furthermore, the use of a fluorescein label allowed excitation in the visible region of the spectrum, eliminating autofluorescence from the cells.

Membrane-Associated Proteins. Another area of increasing importance is the use of membrane-associated proteins for the development of fluorescence-based biosensors. Recent examples include the use of P-glycoprotein (Pgp) to detect drugs and the use of the insulin receptor to detect insulin. The membrane-associated P-glycoprotein was covalently labeled with MIANS at both conserved Cys residues, one within each of the nucleotide binding domains, and was used for the detection of either ATP or drug compounds [54]. ATP bound directly to the labeled nucleotide binding domains of Pgp, causing the fluorescence to be quenched by up to 15% owing to a direct interaction between ATP and the bound probe. Drug compounds, including vinblastine and colchicine, bound to a second site on the protein that was spatially removed from the nucleotide binding site. Drug binding induced a conformational change that resulted in a decrease of up to 60% in the fluorescence intensity. Using this approach, drug compounds could be detected at nanomolar concentrations over a range extending up to 10 μM.

A second example is the use of changes in the intrinsic fluorescence of the insulin receptor (IR) to detect insulin based on an analyte-induced conformational change in the protein [55]. Binding of insulin to IR caused an 35% increase in intrinsic Trp emission intensity, a slight blue shift in the emission maximum, and an increase in the average rotational anisotropy of the protein. These spectroscopic changes were consistent with a change in the average Trp environment in which the probes became somewhat more buried into hydrophobic regions of the protein. The response was sensitive to insulin levels ranging up to 140 nM, and response times ranged from 1 to 20 min, becoming longer as the concentration of insulin decreased. While this particular protein is still far from being useful in an actual sensor, it demonstrates that membrane-associated proteins are candidates for the development of fluorescence-based sensors that rely on analyte-induced conformational changes. Further work will be required to determine if any free Cys residues are available for labeling and if such residues, when labeled, are in locations that are sensitive to changes in protein conformation.

Periplasmic Binding Proteins. Perhaps the most rapidly advancing area of fluorescent biosensor development is the used of fluorescently labeled periplasmic binding proteins (PSPs) for fluorimetric sensing. The first use of this approach was by Cass and co-workers, who examined the effectiveness of a labeled maltose binding protein (MBP) as a maltose sensor [56]. MBP has no native Cys residues but has four methionine residues that could potentially react with thiol selective probes. A single cysteine was used to replace a serine residue at position 337 (S337C), since this position was within the cleft where maltose binding occurred and, hence, experienced a large environmental change on maltose binding. Four thiol-reactive fluorophores were examined: 5-iodoacetoxyfluorescein (IAF), 2-(4′-maleimidylanilino)-naphthalene-6-sulfonic acid (MIANS), 4-[*N*-(iodoacetoxyethyl)-*N*-methylamino]-7-nitrobenz-2-oxa-1,3,-diazole (IANBD), and acrylodan. Neither MIANS nor IAF was found to be sensitive to maltose binding. In the case of MIANS, it was determined that the probe nonselectively labeled the methionine residues, resulting in insensitivity to the conformational change. This result suggested that maleimide derivatives of fluorescent probes may not be ideal for selective labeling of Cys residues when methionine residues are present. IAF was able selectively to label Cys 337, but either blocked ligand binding or interfered with the conformational change.

For both IANBD and Ac, the binding of maltose resulted in a substantial increase in label fluorescence (80% for Ac, 160% for IANBD). Furthermore, the emission wavelength of the Ac label blue-shifted on binding of maltose. These results were consistent with a shift in

the location of the label from a hydrophilic or solvent-exposed environment to a more hydrophobic and buried environment, as would be expected for the closing of the hinge on maltose binding. The IANBD label resulted in an increase in the binding constant of the protein (K_d of unlabeled S337C, 7.7 μM; K_d of IANBD–MBP, 62 μM). In this case, maltose could be detected over a dynamic range of approximately 500 μM, with a limit of detection of approximately 5 μM. In the case of Ac-MBP, there was a decrease in the apparent binding constant, with the K_d being 0.8 μM. In this case, the dynamic range was ca. 3 μM, while the LOD was in the low nanomolar range. These results indicated that the nature of the probe was important in determining the binding behavior of the protein. Both proteins showed association and dissociation rate constants of the order of several hundred seconds which were independent of ligand concentration, indicating that the rate-limiting step in generating a response was likely the conformational change itself.

Webb and co-workers used an engineered phosphate binding protein for the detection of inorganic phosphate (P_i) [57]. In this case, a A197C mutant was prepared and was labeled with the probe *N*-[2-(1-maleimidyl)ethyl]-7-(diethylamino)coumarin-3-carboxamide (MDCC). The fluorescence excitation maximum of this probe is 425 nm, hence the probe is amenable to intracellular studies without problems from autofluorescence. The emission maximum is 474 nm in the absence of P_i but shifts to 464 nm and undergoes a 5.2-fold increase in emission intensity in the presence of saturating amounts of P_i. The new fluorescent protein biosensor was able to detect free P_i over a concentration range from 0 to 0.8 molar equiv of protein with a dissociation constant of 0.3 μM. The response was very fast (under 50 ms) and was remarkably selective. The only compound that proved to be a significant interferant was sodium arsenate, which bound with a K_d of 3 μM. The potential of labeled P_iBP as an arsenate sensor remains to be explored. The rapid response of the new protein-based biosensor has permitted measurements including the release of P_i during ATP hydrolysis by actomyosin subfragment 1 ATPase [57] or myofibril ATPases [58], and during the interaction of p21ras with the GTPase-activating proteins p120–GAP and neurofibromin [59]. In each case, stop-flow measurements were used to follow the reactions and showed that the fluorescently labeled P_i binding protein was able to follow extremely fast processes involving P_i release, which were occurring on the millisecond time scale.

Recent work in the area of fluorescent protein-based biosensors, particularly those involving PBPs, has focused on understanding the mechanism of response and on developing improved strategies for predicting the optimal location of probes within PBPs. With regard to understanding the origin of the analytical signal, most work has endeavored to use time-resolved fluorescence to understand better the changes in the probe environment and photophysics on analyte binding. Three recent examples are presented here. Both Webb and co-workers [60] and Daunert and co-workers [61] have recently reinvestigated the behavior of fluorescently labeled phosphate binding protein using steady-state and time-resolved fluorescence measurements to examine the static and dynamic fluorescence behavior of the protein in the absence and presence of P_i. In both cases, the A197C mutant was used, but in the study by Daunert *et al.*, the protein was labeled with acrylodan, while Webb *et al.* used MDCC.

In the work by Daunert *et al.*, the Ac label was observed to increase in intensity and blue shift upon binding of P_i, consistent with the behavior expected upon P_i induced closure of the binding pocket, which should shield the label from solution, as demonstrated in the earlier work by Webb *et al.* [57]. However, the local motion of the probe was unexpectedly observed to increase on P_i binding, while the apparent accessibility, obtained from the recovered bimolecular quenching rate constant for iodide quenching, indicated greater accessibility of the Ac label in the closed form of the protein. These apparently contradictory results show that the local environment of the probe, including the influence of nearby charged groups, must be carefully considered when attempting to elucidate the factors that are responsible for the fluorescence responses from attached labels. In the case of P_iBP–Ac, it appears that the fluorescence lifetime may in fact be altered on binding of P_i such that the radiative rate constant increases, although no data on fluorescence lifetimes were presented in the paper. If such were the case, the intensity could increase upon binding P_i, even though the probe is more solvent exposed, which would produce a lower nonradiative rate constant. A study of the contributions of radiative and nonradiative contributions to the emission lifetime would be useful in determining the origin of the intensity increase and blue shift in emission wavelength.

In the work by Webb, the MDCC-labeled P_iBP was characterized by steady-state and time-resolved fluorescence [60], combined with x-ray crystallographic data obtained for the labeled protein in the presence and absence of P_i [62]. Fluorescence studies indicated that binding of P_i to the P_iBP–MDCC resulted in an eight fold increase in both quantum yield and fluorescence lifetime for the probe, consistent with the fluorescence changes being induced solely by alterations in the nonradiative rate constant. These changes in steady-state and time-resolved intensity on binding of P_i were accompa-

nied by a decrease in the local rotational mobility and an increase in the global rotational motion of the probe, as determined by time-resolved anisotropy measurements. X-ray crystallography data indicated that the changes in global rotational motion were the result of realignment of the probe from an orientation that was along the minor axis of the protein (which is a prolate ellipsoid) to an orientation that was along the major axis. Overall, the data indicated that the P_i-induced conformational change likely resulted in specific interactions between the diethylamino substituent of the probe and the glycine and alanine residues of the protein. Such an interaction would be expected to depend on both the nature of the probe, the length of the linker chain, and the stereoisomer formed in the labeling reaction. Indeed, all of these factors were observed to have a dramatic effect on the fluorescence sensitivity to P_i-induced conformational changes.

The most remarkable result obtained from the two studies was the large difference in behavior observed simply by changing the probe. These studies clearly shows that a combination of factors, many of which may be unknown, determine the overall sensitivity of fluorescently labeled proteins as reagentless sensors. This result is in agreement with a number of other studies using different labels and proteins and clearly indicates the need for both careful choice of probe and careful investigation of the mechanism of response, in order to optimize a particular protein for sensing of a given analyte.

A final study of reporter group photophysics was that done by Bright and co-workers. This group reinvestigated the utility of fluorescently labeled CaM for sensor development and probed the dynamics of the fluorescent reporter group within the apo and holo forms of the protein [63]. In this case, spinach calmodulin, which has a single Cys at site 26, was site-selectively labeled with a series of thiol-selective probes (acrylodan, fluorescein, and rhodamine) to understand better the basis of the reporter group response. In the case of acrylodan, it was observed that the addition of saturating levels of Ca^{2+} (20 m*M*) to the protein caused a 15% decrease in intensity and a 9-nm red shift in the emission wavelength, consistent with the earlier results reported by Prendergast for Ac-labeled Ca^{2+} binding proteins [45]. The fluorescence intensity of the fluorescein label also decreased, in this case by about 30%, on addition of Ca^{2+}, in agreement with the results of Bachas and co-workers [47], outlined above. It was proposed that this change in signal intensity was the result of a shift in $pK_{a,3}$ for the reaction between the monoanionic (Φ = 0.37) and the dianionic (Φ = 0.93) forms of the probe, resulting in a higher proportion of the monoanion. The basis of the pK_a shift was proposed to be the changes in the relative positions of the many acidic amino acid residues surrounding Cys-26 as a result of the Ca^{2+}-induced change in CaM conformation. The rhodamine label did not show any significant change in emission properties on going from the apo to the holo forms of the protein, consistent with the known insensitivity of rhodamine probes to their local environment. Further investigation of the F-CaM derivative indicated a similar limit of detection compared to randomly labeled F-CaM (ca. 100 nM) but a dynamic range that was almost two orders of magnitude larger than that obtained for the site-selectively labeled protein, extending up to nearly 1.0 m*M*.

The other major advancement in the use of PBPs for sensor development is the use of a "rational design" approach to identify the optimal locations for inserting Cys residues for labeling. The strategy is based on determining the largest difference in residue positions between the apo and the holo crystal structures and selecting these positions for mutations. Hellinga and co-workers used this approach to design an improved mutant of the maltose binding protein for sensor development [64]. A total of six mutants was prepared and labeled, and of these, the Asp95Cys mutant labeled with IANBD was found to be the most sensitive to maltose binding. This mutant produced a 4.4-fold increase in fluorescence intensity when saturated with maltose and could reversibly detect maltose over a range of ca. 10 μM with a LOD of ca. 50 n*M*. The placement of the fluorescent reporter group at a location that was spatially removed from the binding site allowed for the engineering of several mutants wherein Trp residues within the active site (at positions 62, 230, and 340) were individually mutated to alanine residues. The resulting proteins retained similar overall changes in fluorescence intensity on saturation with maltose but showed increased binding constants, ranging from 1.4 μM for the nonmutated D95C protein up to 2800 μM for the D95C/W340A mutant. The addition of maltose to a mixture containing equimolar concentrations of all four mutants showed a dynamic range spanning 0.1 up to 20 m*M*, with an accuracy of 5%. Hence, the ability to engineer not only a fluorescent reporter group site, but also the active site itself, has important advantages for the development of sensors that can span the physiologically relevant range for maltose.

In a second paper, Hellinga and co-workers extended the rational design approach by developing a sensor for glucose [65]. Once again, a number of single Cys mutants were prepared and labeled with either IANBD or Ac. Of all the possible mutant–fluorophore combinations, two were chosen for further study: L255C-Ac and H152C-IANBD. The IANBD label had to be placed directly into

the active site, where a Cys replaces His-152, in order to give a major change in the signal (fourfold). However, this mutation resulted in the dissociation constant increasing by 100-fold. This mutation was beneficial in that it extended the dynamic range for glucose determination up to 100 μM, making it sensitive at the lower portion of the physiological range of glucose concentrations. The Ac label in the L255C mutation was in the hinge region and, thus, was allosterically linked to the binding site. This mutant had a dissociation constant that was only twofold greater than that of the wild-type protein and showed a 50% decrease in intensity and a slight red shift in the emission maximum wavelength on binding of glucose. In this case, the sensor was responsive only over a range of ca. 2 μM, although it had a LOD approaching the low nanomolar range.

It should be noted that while the rational design approach is capable of determining optimal locations for Cys residues, it is clear from the work of Webb *et al.* [60] that the overriding factor that determines the sensitivity of a particular fluorescently labeled protein for sensing of analyte is the nature of the specific interactions between the probe and the amino acid residues of the protein. Thus far, molecular modeling has not proceeded far enough to be able to predict these interactions within proteins, hence the use of a rational design method to optimize the choice of probes is still not possible. This remains a challenge for the future.

Prospects for Reagentless Sensing with Fluorescent Proteins

The advantages of fluorescently labeled proteins for optical sensing of glucose, maltose and other small ligands are many. First, the most obvious advantage is the removal of a requirement for additional reagents to generate a signal. This permits such sensors to be used for "real-time" analysis. Second, such sensors do not consume the analyte, or any other reagent, and hence are reversible. Third, such proteins are not sensitive to any of the normal inhibitors or cofactors that can affect the performance of many enzymes, such as glucose oxidase [66]. Finally, the use of an optical detection strategy removes the potential for electrode fouling, which can seriously affect most electrochemical sensors [67].

Even with these advantages, there are still some precautions that must be taken to obtain a useful protein-based optical biosensor. First, the examples cited above indicate that the technique works best if a single site is selectively labeled. In many cases, selective labeling involves the placement of a Cys residue at a specific location within the protein to allow labeling with a polarity sensitive probe. This approach is limited in that it requires proteins that do not have multiple free thiol groups, since this situation can result in multiple labeling at sites that are not sensitive to protein conformational changes. In some cases it may be possible to remove unwanted residues at the same time that the desired Cys residue is inserted, but one must ensure that these mutations do not irreversibly denature the protein. Second, another potential problem, which has been reported by a number of groups, is that the probe itself may interfere with either ligand binding or the conformational change, producing little or no response to the presence of ligand. However, there are several probes which one can investigate, and usually many positions where the Cys can be located, so that a combination of probe and placement can be found that gives useful analytical performance characteristics. Finally, one must be careful to avoid a situation where the probe is photolabile, since this will result in drastic, irreversible changes in fluorescence intensity which are not related to analyte concentration. Fortunately, there has been progress on the development of sensors that utilize ratiometric signals (anisotropy, FRET, or dual emission probes), and hence this problem can be substantially reduced.

While the current generation of fluorescence-based protein biosensors have shown great promise, there is room for improvement. Fortunately, there are a few recent developments that are likely have a substantial positive impact on the growth of this field. One is the increasing number of methods for site-selectively incorporating fluorescent probes into proteins. For example, in certain cases where an entire protein is not required, it may be possible to use solid-phase synthesis to prepare a suitable peptide, as in the case of the Zn(II)-finger peptides described above [20,43,44]. In such a case, nonnatural amino acids can be selectively placed at any location within the sequence, and one is not restricted to sulfhydryl selective probes. This technique has so far been extended to the preparation of artificial proteins with molecular weights approaching 20 kDa using ligation of oxime-terminated synthetic peptides [68]. In addition, ligation has been successfully used to fuse a small dansyl-labeled peptide between an SH2 and an SH3 domain, resulting in a selectively labeled chimeric protein that underwent an analyte-induced conformational change [69]. The emission of the dansyl probe was sensitive to the binding of branched peptides, showing changes in fluorescence over a range of 500 nM.

Perhaps the most promising approach for selective labeling of larger proteins is the use of chemically aminoacylated tRNA species for *in vitro* expression of mutant proteins with a single nonnatural amino acid placed in

a well-controlled location. Sisido and co-workers [70], following the pioneering work of Schultz [71 and Ross [72], have examined the incorporation of 19 nonnatural aromatic amino acids into streptavidin, including pyrene and anthraquinone derivatized amino acids. Incorporation efficiencies ranged from less than 10% up to greater than 90% and were dependent primarily on the spatial arrangements of the aromatic rings and the number of aromatic rings present. The mutant proteins retained binding affinity for biotin and could be detected by fluorescence methods. Advances in this technique aimed at improving the yields of protein remain a hurdle to be overcome before such proteins can enjoy widespread use for sensor applications. However, given the rapid spread of the more common site-directed mutagenesis techniques, it should be only a matter of time before the *in vitro* expression techniques become more widespread.

ENTRAPMENT OF PROTEINS FOR REAGENTLESS SENSOR DEVELOPMENT

Overview

A number of the proteins described above were used for intracellular studies, including those used for fluorescence ratio imaging. There are numerous other areas where such proteins are particularly useful, such as the continuous monitoring of glucose, insulin, or other physiologically important compounds. To develop self-contained, reuseable, *reagentless* biosensors using the proteins listed above, the biorecognition element has to be put into intimate contact with an optical device to allow transport of excitation radiation to and emission from the biorecognition element. The most common method to achieve this goal is to place the labeled proteins onto or within the surface of an optical fiber or planar waveguide. Typical immobilization strategies have included physical adsorption of the protein onto the surface, various covalent immobilization strategies, and entrapment of the protein either within a semipermeable membrane or into an organic or inorganic polymer matrix [1].

The immobilization step is perhaps the biggest challenge in the development of a working biosensor. A key problem is that many proteins undergo irreversible conformational changes upon interfacing to an inorganic surface, resulting in denaturation and hence loss of biochemical activity. Even in cases where the receptor is successfully immobilized onto the transducer, the complexity of large biomolecules results in a large number of possible orientations in which the protein may adsorb or bind to the transducer. Some proteins may be oriented such that their active sites are not exposed to solution, and thus they will not be able to undergo selective binding reactions. There is also the possibility of time-dependent denaturation of proteins subsequent to immobilization on a surface. In cases where proteins are entrapped, difficulties may include protein denaturation during entrapment and the potential for leaching of the entrapped protein. In all cases, the constantly changing nature of the selective surface leads to an inability to maintain calibration of the sensing device. Even over short periods of time, signal drift may arise from alterations in surface chemistry.

Given the strict requirements for orientational control inherent in the use of many of the proteins described above (particularly the PBPs and membrane-associated proteins), physisorption and covalent attachment strategies are not likely to be successful. However, the entrapment of these species into polymeric matrixes is a promising method for interfacing proteins to inorganic devices. In the past few years, several groups, including our own, have reported on the development and characterization of a new protein interfacing method wherein biological components are encapsulated into inorganic silicate matrixes formed by a low-temperature sol-gel processing method [73–75]. The hydrated glass (sometimes referred to as a bioglass or biogel) contains a significant amount of entrapped water, and as a result, the biologically doped glasses maintain the activity of entrapped compounds such as enzymes [76] and antibodies [77]. A major advantage of these materials is that they are optically transparent, making them ideal for the development of chemical and biochemical sensors that rely on changes in an absorbance or fluorescence signal [78]. Another major advantage of the technique is that it permits coentrapment of multiple species (i.e., proteins, fluorophores, or other reagents) so that only the analyte need enter the glass to generate a signal [79]. Hence, it represents a second possible route to reagentless sensors which does not rely on protein engineering and labeling techniques.

The most common procedure for entrapping proteins into sol-gel processed glass has four stages: acid-catalyzed hydrolysis of an alkoxysilane precursor, such as tetramethylorthosilicate (TMOS) or tetraethylorthosilicate (TEOS), to form a colloidal suspension of silica known as a sol; addition of an aqueous buffer solution containing the protein to promote a large-scale polymerization reaction resulting in gelation; aging of the wet silica network to strengthen the silica network; and partial drying to produce an optically transparent glass material with the protein entrapped in nanometer sized pores. The chemical reactions involved in these steps are shown

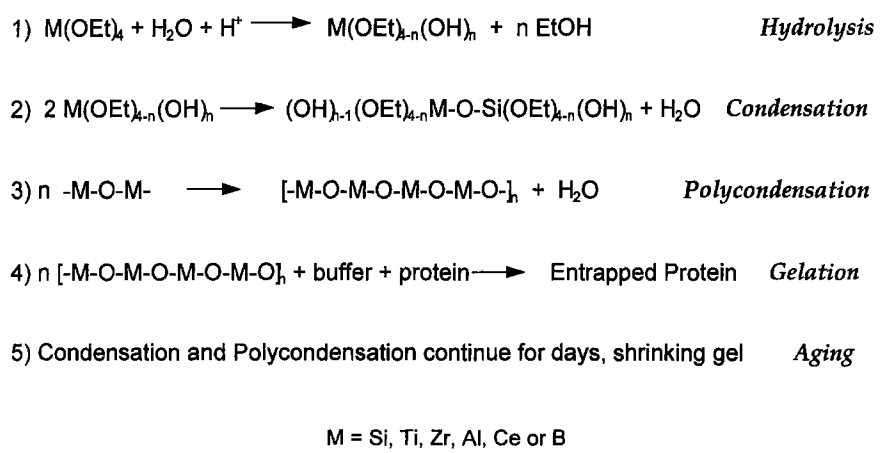

Fig. 3. Reactions involved in the formation of sol-gel-derived glass materials containing entrapped proteins.

schematically in Fig. 3. Interested readers are referred to the works of Brinker and Scherer [80] and Hench and West [81] for a detailed discussion of the sol-gel process and to the reviews by Avnir and co-workers [73] and Zink and co-workers [74] for specific details pertaining to entrapment of biomolecules by this method.

In most research groups, including our own, a "standard" protocol for protein entrapment has evolved [73,74,78]. Normally, sols are prepared by sonicating a mixture of TEOS (or TMOS), water, and 0.1 *N* HCl (typical proportions are 4.5:1.4:0.1, v:v:v) until the mixture becomes clear, colorless, and monophasic. The hydrolyzed TEOS solution is then rapidly mixed with an equal volume of an aqueous buffer solution (typically 10–100 m*M* buffer, pH 7.2, with 100 m*M* KCl, with or without 10–30 μ*M* protein) and immediately placed into a mold, such as a disposable acrylate cuvette, or cast onto the surface of a planar waveguide or optical fiber. Following gelation, the monoliths or films are allowed to age either in buffer (wet aging) [78] or in air (dry aging) [73,74]. During aging, the monoliths can shrink by up to 80% in volume and mass. An advantage of the sol-gel processing method is that it can be used to produce blocks almost any shape or size, depending on the initial dimensions of the mold. In our studies, thin slides were prepared which usually had dimensions of 20 × 5 × 0.2 mm [78].

Conformational Motions of Entrapped Proteins

The most important question regarding entrapped regulatory proteins is whether they remain able to undergo analyte-induced changes in conformation and whether such changes can still be transduced into optical signals. Previous studies have examined the conformational motions and rotational mobility of entrapped proteins using absorbance [82], fluorescence [83–85], and ac impedance [86] measurements. These studies have indicated that the conformational motions of large proteins, such as hemoglobin [82] and bovine serum albumin (BSA) [83,84], can be substantially restricted in sol-gel media. However, small proteins, such as cytochrome *c* [86], appear to be only moderately affected by entrapment.

To determine the effects that entrapment have on the conformational changes associated with ligand binding, our group has examined the effects of entrapment on the properties of the Ca^{2+}-binding protein Cod III parvalbumin (C3P). This protein contains a single Trp residue at position 102 that changes emission characteristics when Ca^{2+} binds. The metal-free (apo) form of the protein is loosely packed. In this form, the quantum yield of the Trp is 0.09 ± 0.01 and the emission wavelength maximum is 335 nm [87,88]. Upon binding of Ca^{2+}, the metal-loaded (holo) structure becomes much more compact. In this case, the quantum yield increases to 0.14 ± 0.01 and the emission wavelength maximum shifts to 315 nm [87].

Figure 4 shows the changes in the Trp emission characteristics of entrapped C3P as a function of Ca^{2+} concentration. Clearly, the emission characteristics change substantially when Ca^{2+} is present, indicating a major change in protein structure. The emission spectra of the apo and holo forms of the entrapped were compared to those of the free protein and were found to be similar. The similarity in the emission spectral characteristics for the free and entrapped apo and holo proteins indicated that the entrapped protein was able fully to undergo Ca^{2+}-induced conformational changes. This was confirmed using fluorescence quenching studies, which showed that

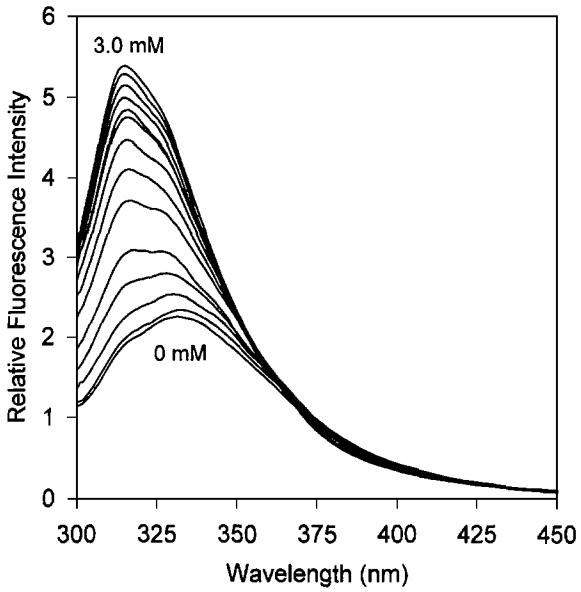

Fig. 4. Fluorescence emission spectra for entrapped Cod III parvalbumin as a function of Ca^{2+}. Excitation was done at 285 nm. The spectra were corrected for background signals and for instrumental distortions.

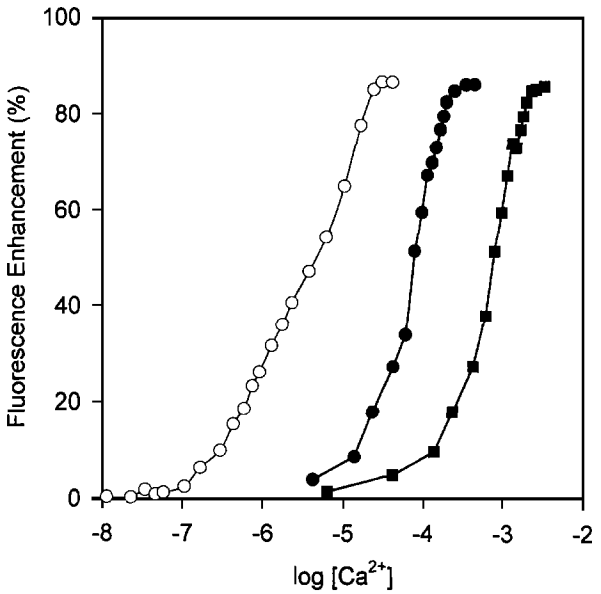

Fig. 5. Changes in integrated fluorescence intensity during the addition of Ca^{2+} to free (○) and entrapped Cod III parvalbumin. Samples containing entrapped C3P were aged for 20 days (●) or 30 days (■). The data are presented as percentage signal enhancement using the integrated intensity of the apo protein as the initial point.

the bimolecular quenching rate constants dropped by a factor of 2 when the entrapped protein went from the apo to the holo form.

Binding Constants of Entrapped Proteins

We have also used fluorescence to determine the binding constants of entrapped metal binding proteins in an effort to determine whether entrapment may affect the dynamic range of such proteins. In this case, three different proteins were examined. The first was cod III parvalbumin. The other two were engineered mutants of rat oncomodulin (OM), which had either a single-residue mutation (Y57W) to place a Trp into the metal binding loop [89] or the complete CD loop replaced by cassette mutagenesis to increase the metal binding affinity [90]. For the OM mutants, the ratio of Tb^{3+} luminescence to Trp fluorescence as a function of the Tb^{3+}:protein molar ratio was used to generate binding curves. For C3P, the change in the integrated intensity of Trp fluorescence was plotted against the Ca^{2+}:protein molar ratio to generate the binding curves. Figure 5 shows examples of binding curves for the free protein and for entrapped C3P obtained 20 days and 30 days after entrapment with the glass slide aged in air. The binding curves clearly showed that entrapment of the protein dramatically altered the binding constant of the protein and that the function of the entrapped protein changed with time. The binding curves obtained for CDOM33 and C3P were analyzed to provide equilibrium binding constants, which were then compared to the values obtained for the proteins in solution. In both cases, the binding constants dropped by approximately five orders of magnitude, from $\sim 10^8\ M^{-1}$ in solution to between 10^3 and $10^4\ M^{-1}$ in the glass. The large changes in the binding constants likely reflected electrostatic interactions between the negatively charged silicate matrix and the negatively charged groups in the binding loops of the proteins and may also have been partially the result of the differences in the properties of entrapped solvents compared to bulk solvents [91,92,93]. The changes in protein function over time represent a major obstacle which remains to be overcome before viable sol-gel-based sensors with extended long-term stability can be produced. However, we have found that storage of monoliths containing Ca^{2+} binding proteins in a Ca^{2+}-loaded aqueous buffer after aging almost completely eliminates this problem and can maintain the function of the entrapped proteins over periods of months.

Prospects for Protein Entrapment for Sensor Development

The development of reagentless fiber-optic sensors based on entrapped fluorescent proteins, such as the PBP family, is still at an early stage. While a wide array of labeled proteins is now available, most have been used

to examine intracellular reactions, and hence there has been very little done in terms of entrapment studies. The few entrapment studies that have been done with such proteins indicate that even though the entrapped proteins remain viable and are able to undergo conformational changes, the placement of the proteins within a porous glass alters the binding affinities of the proteins. Furthermore, entrapment of proteins into glass blocks (referred to as monoliths) results in a large increase in the response times for reactions of proteins with analytes [78,94]. Future studies of sol-gel-entrapped proteins should be done using ultrathin films which are dipcast onto optical fibers. Such a configuration should dramatically reduce response times and should extend the utility of the entrapped protein to the point where remote sensing can be done. Our group is actively pursuing work in this area using both C3P, which is selectively labeled at Cys-18, and spinach calmodulin, which is selectively labeled at Cys-26. The results of these studies will be reported in due course.

CONCLUDING REMARKS

The preparation of fluorescently labeled proteins for reagentless sensor development is now becoming more wide-spread, with a number of new research groups entering this field each year. As more of these species become available, the range of analytes that are amenable to reagentless fluorescence sensing is also increasing. With the emergence of protein-engineering techniques, it is now possible to control not only the location of a dye within a protein, but also the affinity of a protein for its particular analyte. In addition, the development of new labeling methodologies and the use of GFP as a fluorescent label promise to accelerate the rate at which new labeled proteins can be produced. As a result, the time will come when we can design a labeled protein for reagentless sensing of a desired analyte, and this will have a huge impact on the availability and use of fluorescence-based biosensors.

Recently, work has begun in three areas that are of tremendous importance to the progression of this field. The first area is the detailed examination of the photophysical behavior of probes that are bound to the apo and holo proteins. The use of time-resolved fluorescence techniques, combined with studies of probe accessibility, should provide a better understanding of the effects of different probes, and of labeling at different locations, and may lead to a set of guidelines for the preparation of such species. The second area of research is the "rational design" approach for developing fluorescent protein biosensors. This advancement is replacing the first-generation protein reagents, most of which were designed either by random labeling, labeling of a native cysteine, or adding Cys residues in a "hit-and-miss" approach. Newer second-generation reagents will make use of computer prediction tools to aid in determining optimal probe locations. Such techniques may also be able to engineer proteins that have greater stability, extending their utility as components of biosensors. The final area of investigation is the entrapment of such proteins for development of fiber-optic sensors. While a number of possible techniques may eventually be examined to achieve this goal, the use of sol-gel-processed glasses as host matrixes is the most promising method currently under investigation and has shown some important results. Research in this area must focus both on the development of technologies for preparing durable thin films on optical fibers and on improved methods for processing the glass materials so that protein function and stability are maximized and do not change over time. Once these goals are realized, a new generation of fluorescence-based fiber-optic sensors will emerge and will have a major impact on areas such as the understanding of cellular processes, drug screening and discovery, process control, home diagnostic test kits, and remote optical sensing.

ACKNOWLEDGMENTS

I would like to thank the National Sciences and Engineering Research Council of Canada and Research Corporation (Cottrell College Science Award) for financial support of our ongoing work in this area. I would also like to thank C. W. V. Hogue for providing useful comments during the preparation of the manuscript. Finally, I would like to thank K. Flora and L. Zheng, who did the studies on sol-gel-entrapped C3P and OM proteins.

REFERENCES

1. J. Janata, M. Josowicz, P. Vanysek, and D. M. DeVaney (1998) *Anal. Chem.* **70**, 179R–208R.
2. A. J. Cunningham (1998) *Introduction to Bioanalytical Sensors*, John Wiley and Sons, New York.
3. G. E. Boisde and A. Harmer (1996) *Chemical and Biochemical Sensing with Optical Fibers and Waveguides*, Artech House, Norwood.
4. R. Freitag (1996) in R. Freitag (Ed.), *Biosensors and Analytical Biotechnology*, Academic Press, San Diego, pp. 99–127.
5. E. A. H. Hall, J. J. Gooding, and C. E. Hall (1995) *Mikrochim. Acta* **121**, 119–145.
6. L. Regan (1995) *Trends Biochem. Sci.* **20**, 280–285.

7. U. J. Krull, J. D. Brennan, R. S. Brown, S. Hosein, B. D. Hougham, and E. T. Vandenburg (1990) *Analyst* **115**, 147–153.
8. K. A. Guiliano, and D. L. Taylor (1998) *Trends Biotechnol.* **16**, 135–140.
9. M. Thompson and U. J. Krull (1991) *Anal. Chem.* **63**, 393A–405A.
10. P. Fabry and E. Siebert (1997) in P. J. Gellings and H. J. M. Bouwmeester (Eds.), *CRC Handbook of Solid State Electrochemistry*, CRC Press, Boca Raton, FL, pp. 329–369.
11. A. Izquierdo and M. D. Luque de Castro (1995) *Electroanalysis* **7**, 505–519.
12. J. W. Grate, S. J. Martin, and R. M. White (1993) *Anal. Chem.* **65**, 940A.
13. G. C. M. Meijer and A. W. van Herwaarden (1994) *Thermal Sensors*, Institute of Physics, Bristol, UK.
14. R. A. Potyrailo, S. E. Hobbs, and G. M. Hieftje (1998) *Anal Chem.* **70**, 1639–1645.
15. I. R. Lewis and P. R. Griffiths (1996) *Appl. Spectrosc.* **50**, 12A–30A.
16. M. Malmqvist (1996) in H. C. Hoch, L. W. Jelinski, and H. G. Craighead (Eds.), *Nanofabricated Biosystems*, Cambridge University Press, Cambridge, pp. 103–122.
17. G. Gauglitz (1996) *Sens. Update* **1**, 1–45.
18. R. B. Thompson, B. P. Maliwal, V. L. Feliccia, C. A. Fierke, and K. McCall (1998) *Anal. Chem.* **70**, 4717–4723.
19. F. V. Bright, T. A. Betts, and K. S. Litwiler (1990) *Anal. Chem.* **62**, 1065–1069.
20. G. Walkup, and B. Imperiali (1996) *J. Am. Chem. Soc.* **118**, 3053–3054.
21. G. Weber (1966) in E. C. Slater (Ed.), *Flavin and Flavoproteins*, Elsevier, New York, pp. 15–21.
22. A. Visser (1984) *Photochem. Photobiol.* **40**, 703–706.
23. O. S. Wolfbeis and W. Trettnak (1989) *SPIE* **1172**, 287–292.
24. W. Trettnak and O. S. Wolfbeis (1989) *Anal. Chim. Acta* **221**, 195–203.
25. W. Trettnak and O. S. Wolfbeis (1989) *Fresnius Z. Anal. Chem.* **334**, 427–430.
26. A. M. Harnett, C. M. Ingersoll, G. A. Baker, and F. V. Bright (1999) *Anal. Chem.* **71**, 1215–1224.
27. R. B. Thompson and E. R. Jones (1993) *Anal Chem.* **65**, 730–734.
28. D. Elbaum, S. K. Nair, M. W. Patchan, R. B. Thompson, and D. W. Christianson (1996) *J. Am. Chem. Soc.* **118**, 8381–8387.
29. R. B. Thompson, and B. P. Maliwal (1998) *Anal. Chem.* **70**, 1749–1754.
30. R. B. Thompson, B. P. Maliwal, V. L. Feliccia, C. A. Fierke, and K. McCall (1998) *Anal. Chem.* **70**, 4717–4723.
31. C. M. Hanbury, W. G. Miller, and R. B. Harris (1997) *Clin. Chem.* **43**, 2128–2136.
32. C. L. Morgan, D. J. Newman, and C. P. Price (1996) *Clin. Chem.* **42**, 193–209.
33. B. Hock (1997) *Anal. Chim. Acta* **347**, 177–186.
34. R. T. Piervincenzi, W. M. Reichert, and H. W. Hellinga (1998) *Biosens. Bioelectron.* **13**, 305–312.
35. J. D. Stewart, V. A. Roberts, M. W. Crowder, E. D. Getzoff, and S. J. Benkovic (1994) *J. Am. Chem. Soc.* **116**, 415–416.
36. G. V. Richieri, R. T. Ogata, and A. M. Kleinfeld (1992) *J. Biol. Chem.* **267**, 23495–23501.
37. P. L. Post, K. M. Trybus, and D. L. Taylor (1994) *J. Biol. Chem.* **269**, 12880–12887.
38. S. L. Barker, R. Kopelman, T. E. Meyer, and M. A. Cusanovich (1998) *Anal. Chem.* **70**, 971–976.
39. M. Gerstein, A. M. Lesk, and C. Chothia (1994) *Biochemistry* **33**, 6739–6749.
40. K. A. Giuliano, P. L. Post, K. M. Hahn, and D. L. Taylor (1995) *Annu. Rev. Biophys. Biomol. Struct.* **24**, 405–434.
41. H. W. Hellinga and J. S. Marvin (1998) *Trends Biotechnol.* **16**, 183–189.
42 A. M. Lesk and C. Chothia (1988) *Nature* **335**, 188–190.
43. G. K. Walkup and B. Imperiali (1997) *J. Am. Chem. Soc.* **119**, 3443–3450.
44. H. A. Godwin and J. M. Berg (1996) *J. Am. Chem. Soc.* **118**, 6514–6515.
45. F. G. Prendergast, M. Meyer, G. L. Carlson, S. Iida, and J. D. Potter (1983) *J. Biol. Chem.* **258**, 7541–7543.
46. K. M. Hahn, A. S. Waggoner, and D. L. Taylor (1990) *J. Biol. Chem.* **265**, 20335–20345.
47. T. L. Blair, S.-T. Yang, T. Smith-Palmer, and L. G. Bachas (1994) *Anal. Chem.* **66**, 300–302.
48. J. A. Putkey, W. Liu, X. Lin, S. Ahmed, M. Zhang, J. D. Potter, and W. G. L. Kerrick (1997) *Biochemistry* **36**, 970–978.
49. R. Y. Tsien and A. Miyawaki (1998) *Science* **280**, 1954–1955.
50. V. A. Romoser, P. M. Hincle, and A. Persechini (1997) *J. Biol. Chem.* **272**, 13270–13274.
51. A. Persechini, J. A. Lynch, and V. A. Rosomer (1997) *Cell Calcium* **22**, 209–216.
52. A. Miyawaki, J. Liopis, R. Helm, J. M. McCaffery, J. A. Adams, M. Ikura, and R. Y. Tsein (1997) *Nature* **388**, 882–887.
53. S. R. Adams, A. T. Harootunian, Y. J. Buechler, S. S. Taylor, and R. Y. Tsien (1991) *Nature* **349**, 694–697.
54. R. Lui and J. Sharom (1996) *Biochemistry* **35**, 11865–11873.
55. J. Lee, P. F. Pilch, S. E. Shoelson, and S. F. Scarlata (1997) *Biochemistry* **36**, 2701–2708.
56. G. Gilardi, L. Q. Zhou, L. Hibbert, and A. E. G. Cass (1994) *Anal. Chem.* **66**, 3840–3847.
57. M. Brune, J. L. Hunter, J. E. T. Corrie, and M. R. Webb (1994) *Biochemistry* **33**, 8262–8371.
58. C. Lionne, M. Brune, M. R. Webb, F. Travers, and T. Barman (1995) *FEBS Lett.* **364**, 59–62.
59. A. E. Nixon, M. Brune, P. N. Lowe, and M. R. Webb (1995) *Biochemistry* **34**, 15592–15598
60. M. Brune, J. L. Hunter, S. A. Howell, S. R. Martin, T. L. Hazlett, J. E. T. Corrie, and M. R. Webb (1998) *Biochemistry* **37**, 10370–10380.
61. J. S. Lundgren, L. L. E. Salins, I. Kaneva, and S. Daunert (1999) *Anal. Chem.* **71**, 589–595.
62. M. Hirshberg, K. Hendrick, L. L Haire, N. Vasisht, M. Brune, J. E. T. Corrie, and M. R. Webb (1998) *Biochemistry* **37**, 10381–10385.
63. A. N. Watkins and F. V. Bright (1998) *Appl. Spectrosc.* **52**, 1447–1456.
64. J. S. Marvin, E. E. Corcoran, N. A. Hattangadi, J. V. Zhang, S. A. Gere, and H. W. Hellinga (1997) *Proc. Natl. Acad. Sci. USA* **94**, 4366–4371.
65. J. S. Marvin and H. W. Hellinga (1998) *J. Am. Chem. Soc.* **120**, 7–11.
66. P. Audebert, C. Demaille, and C. Sanchez (1993) *Chem. Mater.* **5**, 911–913.
67. D. A. Gough and J. C. Armour (1995) *Diabetes* **44**, 1005–1009.
68. K. Rose (1994) *J. Am. Chem. Soc.* **116**, 30–33.
69. G. J. Cotton, B. Ayers, R. Zu, and T. W. Muir (1999) *J. Am. Chem. Soc.* **121**, 1100–1101.
70. T. Hahsaka, K. Kajihara, Y. Ashizuka, J. Murakami, and M. Sisido (1999) *J. Am. Chem. Soc.* **121**, 34–40.
71. D. Mendel, V. W Cornish, and P. G. Schultz (1995) *Annu. Rev. Biophys. Biomol. Struct.* **24**, 435–462.
72. L. E. Steward, C. S. Collins, M. A. Gilmore, J. E. Carlson, J. B. A. Ross, and A. R. Chamberlin (1997) *J. Am. Chem. Soc.* **119**, 6–11.
73. D. Avnir, S. Braun, O. Lev, and M. Ottolenghi (1994) *Chem. Mater.* **6**, 1605–1614.
74. B. C. Dave, B. Dunn, J. S. Valentine, and J. I. Zink (1994) *Anal. Chem.* **66**, 1120A–1126A.
75. J. D. Brennan (1999) *Appl. Spectrosc.* **53**, in press.
76. Q. Chen, G. L. Kenausis, and A. Heller (1998) *J. Am. Chem. Soc.* **120**, 4582–4585.
77. A. Bronshtein, N. Aharonson, D. Avnir, A. Turniansky, and M. Altstein (1997) *Chem. Mater.* **9**, 2632–2639.
78. L. Zheng, W. R. Reid, and J. D. Brennan (1997) *Anal. Chem.* **69**, 3940–3949.
79. S. A. Yamanaka, F. Nishida, L. M. Ellerby, C. R. Nishida, B. Dunn, J. S. Valentine, and J. I. Zink (1992) *Chem. Mater.* **4**, 495–497.

80. C. J. Brinker and G. W. Scherer (1989) *Sol-Gel Science*, Academic Press, New York.
81. L. L. Hench and J. K. West (1990) *Chem. Rev.* **90**, 33–72.
82. N. Shibayama and S. Saigo (1995) *J. Mol. Biol.* **251**, 203–209.
83. P. L. Edmiston, C. L. Wambolt, M. K. Smith, and S. S. Saavedra (1994) *J. Coll. Int. Sci.* **163**, 395–406.
84. J. D. Jordan, R. A. Dunbar, and F. V. Bright (1995) *Anal. Chem.* **67**, 2436–2443.
85. K. K. Flora and J. D. Brennan, (1998) *Anal. Chem.* **70**, 4505–4513.
86. B. C. Dave, H. Soyez, J. M. Miller, B. Dunn, J. S. Valentine, and J. I. Zink (1995) *Chem. Mater.* **7**, 1431–1434.
87. C. M. L. Hutnik, J. P. MacManus, and A. G. Szabo (1990) *Biochemistry* **29**, 7318–7328.
88. C. M. L. Hutnik, MacManus, D. Banville, and A. G. Szabo (1990) *J. Biol. Chem.* **265**, 11456–11464.
89. J. P. MacManus, C. M. L. Hutnik, B. D. Sykes, A. G. Szabo, T. C. Williams, and D. Banville (1988) *J. Biol. Chem.* **264**, 3470–3477.
90. I. D. Clark, A. J. Bruckman, C. W. V. Hogue, J. P. MacManus, and A. G. Szabo (1994) *J. Fluoresc.* **4**, 235–241.
91. C. Shen and N. M. Kostic (1997) *J. Am. Chem. Soc.* **119**, 1304–1312.
92. S. Xu, L. Ballard, Y. J. Kim, and J. Jonas (1995) *J. Phys. Chem.* **99**, 5787–5792.
93. J.-P. Korb, A. Delville, S. Xu, G. Demeulenaere, P. Costa, and J. Jonas, (1994) *J. Chem. Phys.* **101**, 7074–7081.
94. L. Zheng, K. Flora, and J. D. Brennan (1998) *Chem. Mater.* **10**, 3974–3983.